Dynamics of a Polymer Solution in a Rigid Matrix. 2

Carmen Kloster,[†,‡] Clara Bica,[‡] Cyrille Rochas,[†] Dimitrios Samios,[‡] and Erik Geissler*[,†]

Laboratoire de Spectrométrie Physique, CNRS UMR 5588, B.P. 87, 38402 St Martin d'Hères Cedex, France, and Laboratorio de Instrumentação e Dinâmica molecular, Instituto de Quimica, Universidade Federal do Rio Grande do Sul, Porto Alegre, Bento Gonçalves 9500, Rio Grande do Sul, Brazil

Received November 30, 1999; Revised Manuscript Received June 1, 2000

ABSTRACT: Dynamic light scattering measurements of the diffusion coefficient D and the Rayleigh ratio R_θ are reported for dextran molecules confined in agarose gel networks of various concentrations. In this condition, the light scattered by the dextran is some 2 orders of magnitude less intense than that from the agarose. Three molecular weights of dextran were investigated: 7×10^4, 5×10^5, and 2×10^6 g mol^{-1}. For the lowest molar mass it is confirmed that, below the dextran overlap concentration c^*, the product DR_θ is independent of the agarose concentration, showing that the reduction of the rate of diffusion inside the gel is the result of a decrease in the osmotic pressure in the confined geometry. For the higher molar masses, entanglement effects between the dextran and the network become noticeable in the more highly concentrated gels. The dynamic light scattering intensity measurements are also found to yield reasonable estimates of the molar mass M_w and radius of gyration R_G of the trapped dextran molecules. The second virial coefficient A_2 is positive, indicating that the agarose−water matrix acts as a good solvent for dextran, but the ratio of R_G to the hydrodynamic radius is less than 1.5. These results are interpreted in terms of branching of the dextran molecule.

Introduction

Over the past two decades, a number of investigations have been made into the diffusion of probe particles inside polymer solutions and gels using dynamic light scattering.[1−8] Recently, we extended this technique to include measurements of the intensity of the scattered light, applied to low molar mass dextran solutions ($M_w \approx 70\,000$ g mol^{-1}) trapped inside agarose gels.[9] In this system, the two components are miscible over a limited concentration range, above which the gel that is formed displays phase separation on a macroscopic scale. In the range of miscibility the dextran molecules migrate freely throughout the volume of the sample that is not occupied by the agarose, and their behavior is therefore similar to that of a liquid. The light scattered by the gel structure itself was found to be some 2 or 3 orders of magnitude more intense than that scattered by the mobile macromolecules, with the result that the latter was strongly heterodyned. In this situation, photon correlation spectroscopy can be used to discriminate between these two components since, in the concentration range of interest, agarose gels are virtually immobile at room temperature; in the pure gel residual motions were found to scatter between 0.01 and 0.05% of the total light, depending on the agarose concentration. In this system, then, the only significant dynamic component is that of the mobile guest polymer. Analysis of the resulting intensity correlation functions accordingly yields not only the corresponding diffusion coefficient D but also the Rayleigh ratio R_θ.

The results of ref 9 may be summarized as follows. For concentrations below the overlap concentration c^*, the diffusion coefficient D of the dextran in the gel is depressed with respect to the free solution. Conversely, the intensity R_θ scattered by the trapped molecules is enhanced over that in the free state. The product of these two quantities, DR_θ, however, was found to depend only on the dextran concentration c and to be independent of the gel concentration c_g. These results showed that the reduction in diffusion rate is not due to frictional effects but instead comes from a depression of the osmotic pressure due to configurational entropy loss in the confined volume of the gel.

It is natural to try to extend these observations to larger guest molecules in order to explore larger length scales in the gel. For this reason, in this article we report measurements on agarose gels containing dextran solutions of higher molar mass, namely 5×10^5 and 2×10^6 g mol^{-1}, the radii of gyration R_G of which are appreciably larger.

Experimental Section

The sample preparation was described in detail in ref 9. Three lots of dextran, of molar mass $M_w = 7 \times 10^4$, 5.0×10^5, and 2.0×10^6 g mol^{-1}, were used as supplied by Sigma. The molar mass of the agarose, kindly provided by R. Armisen (Hispanagar, Spain), was $M_w = 1.2 \times 10^5$ g mol^{-1} (sulfate content 0.1%, methyl content 0.6%). Previous measurements[10] of the molar mass of these samples yielded the results displayed in Table 1.

The appropriate weights of agarose and dextran were mixed in deionized water and heated to 100 °C and stirred to complete dissolution. The solutions were sealed in 10 mm diameter cylindrical glass tubes, then melted again at 100 °C, and allowed to cool to room temperature. Gelation of the agarose occurred as the temperature fell to 45 °C.

Dextran and agarose form uniform gels in water over a limited concentration range, above which macroscopic phase separation occurs. The phase diagram is shown in Figure 1. The experiments described in this article were all conducted in the region of miscibility.

Dynamic light scattering measurements were made with a Spectra Physics SP1161 laser working at 488 nm and a Malvern Instruments 7032 multibit correlator. All measurements were made in a temperature-controlled bath at 25 °C.

[†] Laboratoire de Spectrométrie Physique.
[‡] Laboratorio de Instrumentação e Dinâmica molecular.

10.1021/ma992005q CCC: $19.00
Published on Web 07/29/2000

Table 1. Light Scattering Parameters for Dextran

M_{nom}/1000	M_w/1000	R_G/nm	R_H/nm	$\rho = R_G/R_H$	A_2/cm^3 mol g^{-2}	remarks
70	64	9.6	6.5	1.48		ref 10, $c_g = 0$ g L^{-1}
500	490	24.4	16	1.53		ref 10, $c_g = 0$ g L^{-1}
2000	1850	42.2	37.8	1.12		ref 10, $c_g = 0$ g L^{-1} (fraction from chromatography column)
70			6.2			this work, $c_g = 0$ g L^{-1}
70			7.8			this work, $c_g = 5$ g L^{-1}
500	540	23.1	18.7	1.24	2.5×10^{-4}	this work, $c_g = 5$ g L^{-1}
2000	3400	59.8	43	1.39	7.3×10^{-5}	this work, $c_g = 5$ g L^{-1}
2000	2900	42.5	55.9	0.76	7.3×10^{-5}	this work, $c_g = 10$ g L^{-1}

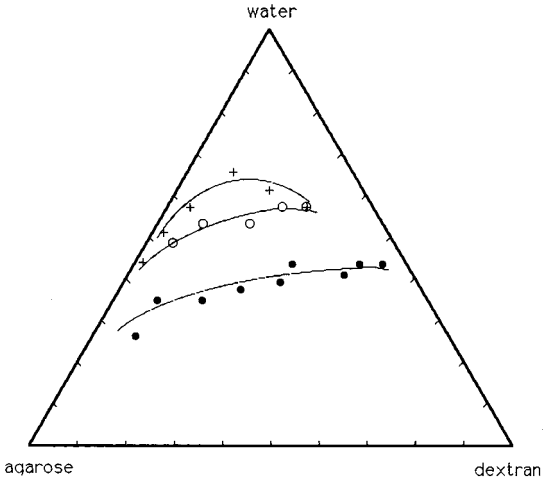

Figure 1. Expanded view of the phase diagram of the agarose−dextran−water system, for the three molar masses studied. Filled circles, $M = 7 \times 10^4$ g mol^{-1}; open circles, $M = 5 \times 10^5$ g mol^{-1}; crosses, $M = 2 \times 10^6$ g mol^{-1}. The phase-separated region lies below the curves indicated. The scale in the diagram is agarose: 0−10% w/w, dextran 0−10% w/w, water 90−100% w/w.

The laser and goniometer were fixed to an optical table that was isolated from the building by pneumatic supports.

The optical transmission factors T_s of the samples were measured in the same cells, using a Kontron Uvikon 810 spectrophotometer working at 488 nm. To compensate for the lens effect of the cylindrical light scattering tubes, these were placed in rectangular spectrophotometric cells containing water in the intervening space. A mask was applied to ensure that only light traversing the cylinder diameter was detected by the spectrophotometer.

For the free solutions of dextran, the scattered light consists entirely of the fluctuating component, I_f, and dynamic light scattering measurements were made in the usual homodyne condition.[11] For solutions trapped in the gels, however, the rigid agarose structure adds a static component of stray light I_s which generates heterodyne mixing at the photomultiplier. The total average scattering intensity is then

$$\langle I \rangle = \langle I_f + I_s \rangle \tag{1}$$

and the resulting normalized intensity correlation function is[12]

$$G(\tau) = G(\infty) + \beta[2X(1 - X)g(\tau) + X^2 g^2(\tau)] \tag{2}$$

In eq 2, $X = \langle I_f \rangle / \langle I \rangle$ is the fluctuating fraction of the scattered light, β is the optical coherence factor of the detection system, and $g(\tau)$ is the field correlation function of the fluctuating component. The quantity

$$G(\infty) = \frac{\langle I_s^2 \rangle + 2\langle I_s \rangle \langle I_f \rangle + \langle I_f \rangle^2}{\langle I \rangle^2} \tag{3}$$

is the value of $G(\tau)$ at the far point, generally set to be 2048 times the longest time increment in the correlation window.

As noted by Joosten et al.,[13] eq 2 is soluble both for X and for $g(\tau)$, since, by definition, $g(0) = 1$. From these results the Rayleigh ratio of the fluctuating component of the scattered light R_θ can in turn be evaluated, giving[9]

$$R_\theta = \frac{R_v X \langle I \rangle \sin \theta}{I_{stand} T_s} \tag{4}$$

where R_v is the Rayleigh ratio of the toluene standard and I_{stand} the intensity scattered by the standard in the same conditions of incident laser intensity as the sample.

The diffusion coefficient D is obtained from the field correlation function. In general, this can be described by a multiexponential decay

$$g(\tau) = \sum_1^N a_n \exp(-D_n q^2 \tau) \tag{5}$$

which yields the z-average diffusion coefficient

$$D_z = -\frac{1}{q^2} \partial \ln g(\tau)/\partial\tau = \sum_1^N a_n D_n / \sum_1^N a_n \tag{6}$$

For the two lower molar mass samples investigated here (7×10^4 and 5×10^5 g mol^{-1}), satisfactory fits to the results were found for $N = 2$, and this analysis was accordingly adopted throughout. In the former of these samples the contribution of the slower relaxation to D_z was small (ca 1%). The samples of molar mass 2×10^6 g mol^{-1}, however, required three components for a satisfactory description, both in the free solution and inside the gel; as mentioned below, this sample displays greater polydispersity, which is probably sufficient to explain the observed distribution of relaxation times.

Despite the essentially static character of I_s, the correlation functions did sometimes show evidence of residual movement of the speckle pattern, presumably owing to mechanical relaxation of the sample in response to small temperature changes in the thermostated bath. As such changes occur on a time scale much longer than that of the diffusion of the guest polymer, their contribution could be eliminated simply by replacing $G(\infty)$ in eq 2 by the value of $G(\tau)$ in the last correlator channels where the correlation function of the polymer is fully relaxed.

Results and Discussion

Figure 2 shows examples of the normalized intensity correlation functions measured at a scattering angle of 90° for two samples containing 15 g L^{-1} of dextran of mass 5×10^5 g mol^{-1}, in aqueous solution and inside a hydrogel composed of 30 g L^{-1} agarose. For visibility, the latter has been multiplied by a factor of 100. The corresponding field correlation functions $g(\tau)$, calculated from eq 2, are shown in Figure 3, together with the corresponding two-exponential fits through the data points. In Figure 4a the resulting relaxation rates

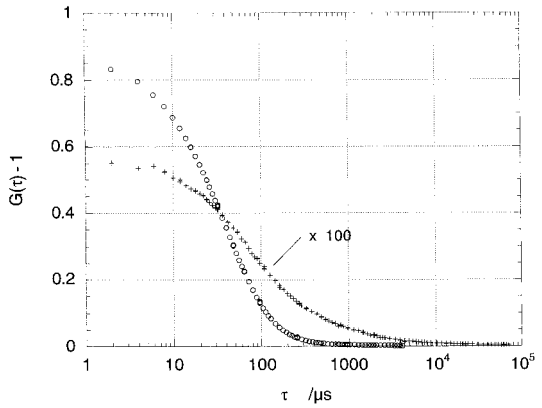

Figure 2. Intensity correlation functions $G(\tau) - 1$ for an dextran solution ($M = 5 \times 10^5$) at $c = 15$ g/L at $\theta = 90°$ in free solution (open circles) and in a $c_g = 30$ g/L agarose gel (crosses). For visibility, the latter is multiplied by a factor 100.

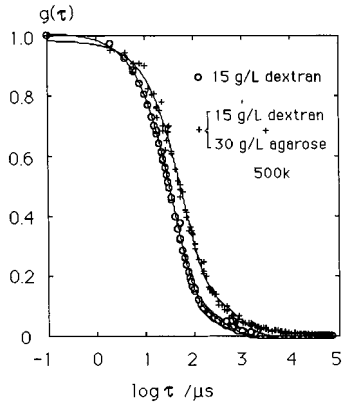

Figure 3. Field correlation functions $g(\tau)$ calculated from Figure 2 using eq 2.

$$\Gamma = D_z q^2 \tag{7}$$

are shown as a function of q^2, for a set of samples with dextran concentration $c = 10$ g L^{-1} in three different agarose environments: $c_g = 0$, 5, and 30 g L^{-1}. Each data set gives a straight line through the origin, in agreement with eq 7. This linear behavior is consistent with that found earlier[1] for dextran of molar mass 7×10^4 g mol^{-1}.

Figure 4b shows that the linear relationship 7 also holds for the 2×10^6 molar mass solutions inside agarose gels. For this high molar mass sample, however, there is evidence of aggregation in the free solution: the scattering intensity displays an increase at low angles that is incompatible with the stated value of the mass. For this reason comparative measurements are made between the free solution and the gels using the data from $\theta = 150°$. The resulting values of $D_z(c)$ are shown in Figure 5a−c as a function of agarose concentration c_g, for the three different molar masses M investigated. The behavior of each set of samples is similar. At low dextran concentrations c, D_z is depressed by an amount that accentuates with increasing c_g; at higher c this effect disappears, and the $D_z(c)$ curves converge in the vicinity of $c = 40$ g L^{-1}.

The Rayleigh ratio R_θ, shown in Figure 6 for the different molar masses investigated, also displays behavior similar to that of the $M = 7 \times 10^4$ g mol^{-1} system (Figure 6a). Contrary to the diffusion coefficient, R_θ is higher inside the gel than in free solution. For $M = 5 \times 10^5$ g mol^{-1} the angular variation of R_θ is weak, and it

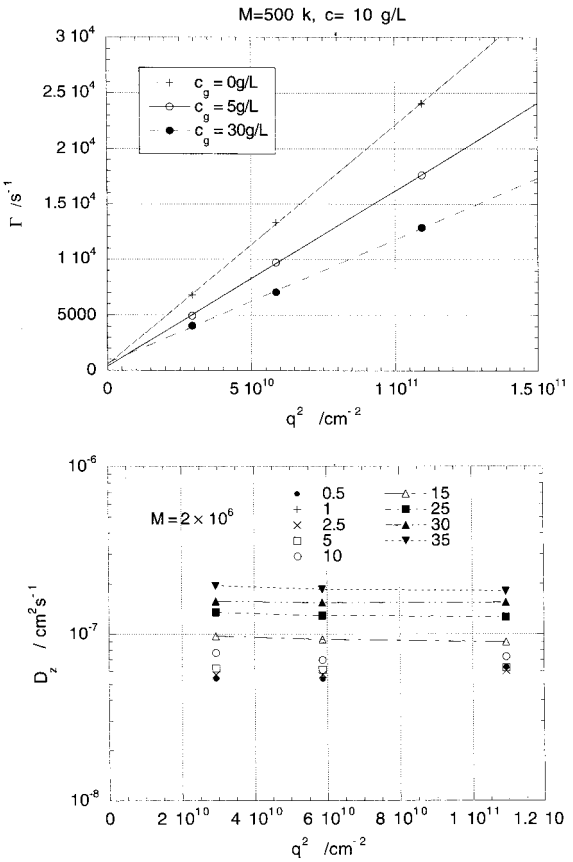

Figure 4. (a) Relaxation rate Γ of the field correlation function $g(\tau)$ as a function of q^2 for a $c = 10$ g L^{-1} dextran solution of molar mass 5×10^5 g mol^{-1}: crosses, free solution; open circles, inside an agarose gel with $c_g = 5$ g L^{-1}; filled circles, inside an agarose gel with $c_g = 30$ g L^{-1}. (b) Diffusion coefficient $D_z = \Gamma/q^2$ for the 2×10^6 g mol^{-1} dextran in an agarose gel with $c_g = 5$ g L^{-1}, at various dextran concentrations c between 0.5 and 35 g L^{-1}. For these samples, D_z is independent of q.

is reasonable to plot the average value for the three angles as in Figure 6b. For $M = 2 \times 10^6$, to minimize the effects of aggregation in the free solutions, Figure 6c shows the variation of R_{150} only.

It is known from basic physical principles[14,15] the quantities D_z and R_θ are both functions of the osmotic susceptibility $\partial c/\partial \Pi$:

$$D_z = \frac{\partial \Pi/\partial c}{f} \tag{8}$$

$$R_\theta = Kc\,\frac{kT}{\partial \Pi/\partial c} \tag{9}$$

where f is a friction coefficient that, in the dilute regime, corresponds to that of the whole molecule. K is the contrast factor for light scattering. From eqs 8 and 9 it follows that the product

$$D_z R_\theta = KkTc/f \tag{10}$$

is independent of the thermodynamic quantity Π.

Figure 7 shows the product $D_z R_\theta$ for the three sets of samples. As found previously,[9] the points for the lowest mass fall on a plausible master curve. This result implies that frictional coupling between the dextran and the gel is negligible. For the two higher masses, however, the increase in R_θ does not completely compensate for the depression in D_z, evoking a slowing effect

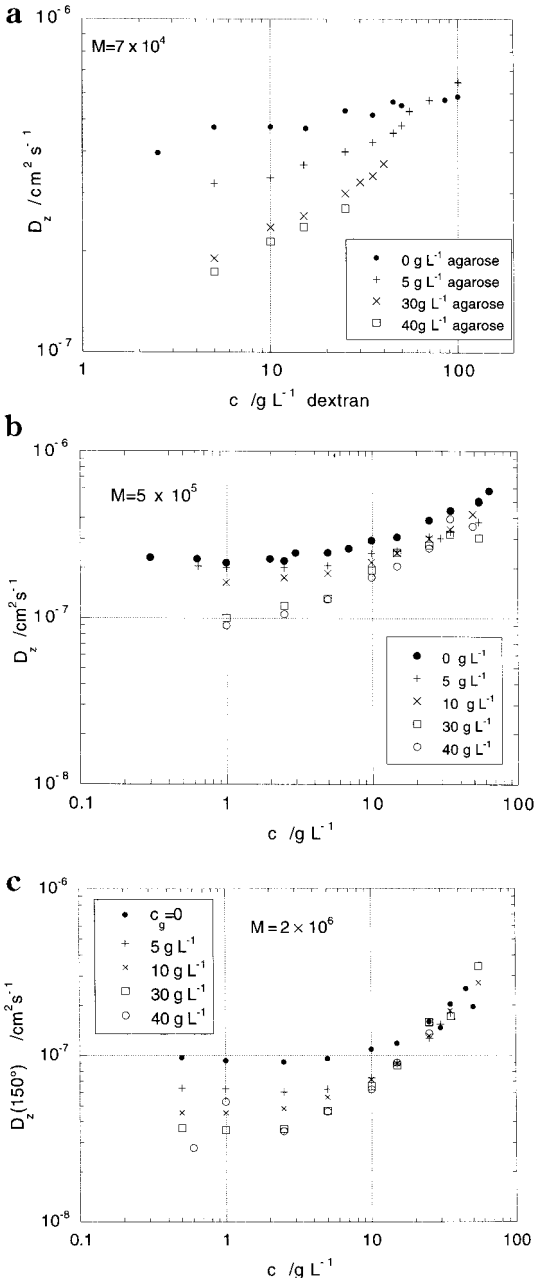

Figure 5. Diffusion coefficient D_z as a function of dextran concentration c in agarose gels of various concentrations c_g: (a) $M = 7 \times 10^4$ g mol^{-1}, (b) $M = 5 \times 10^5$ g mol^{-1}, (c) $M = 2 \times 10^6$ g mol^{-1} (measured at $\theta = 150°$).

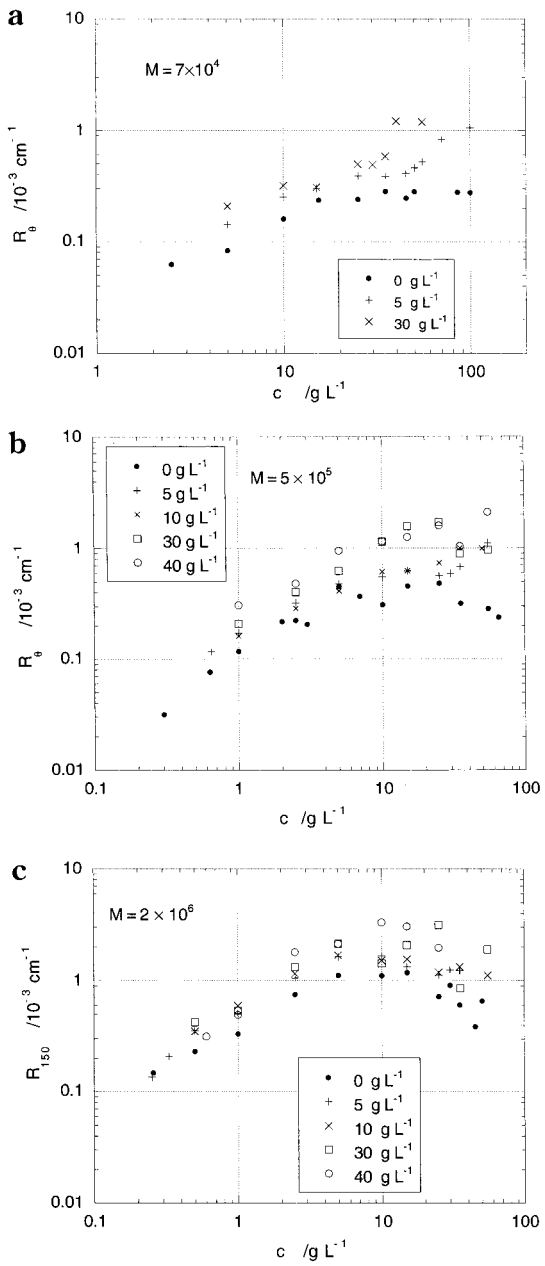

Figure 6. Rayleigh ratio R_θ as a function of dextran concentration c in agarose gels of various concentrations c_g: (a) $M = 7 \times 10^4$ g mol^{-1}, (b) $M = 5 \times 10^5$ g mol^{-1}, (c) $M = 2 \times 10^6$ g mol^{-1} (measured at $\theta = 150°$).

of nonthermodynamic origin that preferentially affects the larger masses. A likely explanation for this slowing is the existence of entanglements between the dextran and the rigid matrix. Such an effect should be more marked at higher agarose concentrations, where the pore size of the matrix is smaller.[16] [The notion of pore size is not entirely appropriate in agarose gels, as the structure is characterized by an extremely broad distribution of distances.[17] The intensity maximum observed in small-angle light scattering can, however, be taken as an indication of a maximum pore size.] Moreover, returning to Figure 6a−c elicits another observation: as the molecular weight increases, the enhancement of R_θ by the agarose network weakens. It seems probable that this effect is the result of territorial competition between the dextran and the agarose as the gel forms. Under such conditions the agarose network is deformed locally and the dextran molecules have a greater degree of freedom than if they were introduced after the formation of the gel. This result has important implications for the configuration of the guest molecules.

We now turn to the angular dependence of R_θ. Traditionally, the molar mass M_w and radius of gyration R_G of molecules in solution are determined by static light scattering. In aqueous solutions such measurements are notoriously difficult owing to the extreme precautions that have to be taken to eliminate dust and molecular associations. In the present case, however, these sources of stray light are immobilized inside the agarose gels, contributing a signal that simply adds to the already strong static light background. It is therefore not unreasonable that the values of R_θ obtained by dynamic light scattering should provide valid information on the characteristics of the dissolved dextran molecules. Results for the three angles investigated are illustrated in parts a and b of Figure 8 as Zimm plots

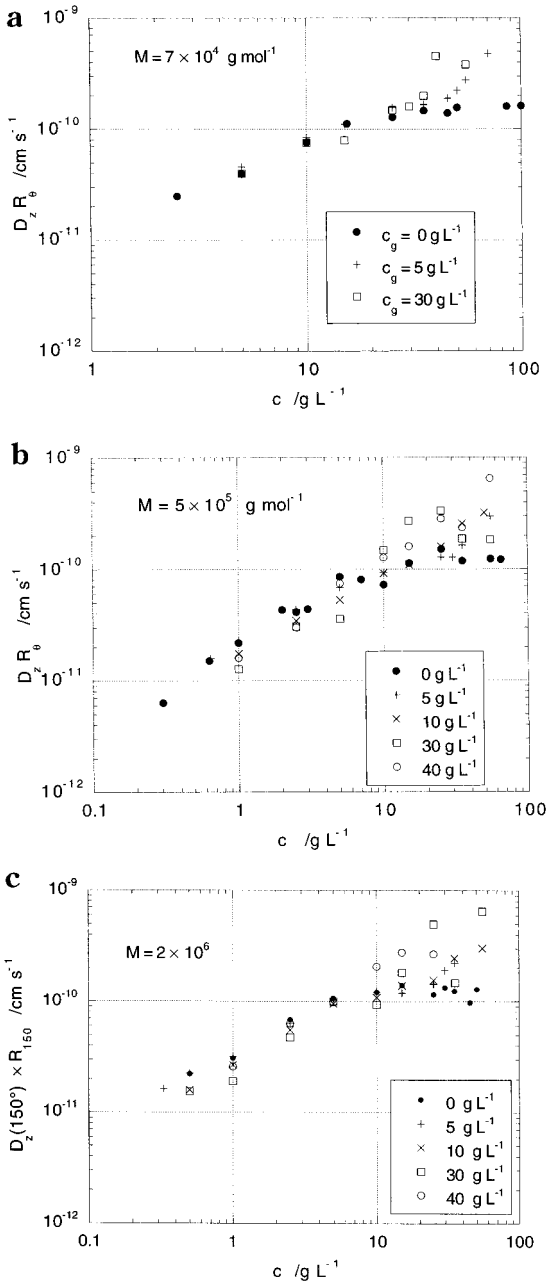

Figure 7. D_zR_θ as a function of dextran concentration c in agarose gels of various concentrations c_g: (a) $M = 7 \times 10^4$ g mol^{-1}, (b) $M = 5 \times 10^5$ g mol^{-1}, (c) $M = 2 \times 10^6$ g mol^{-1} (measured at $\theta = 150°$).

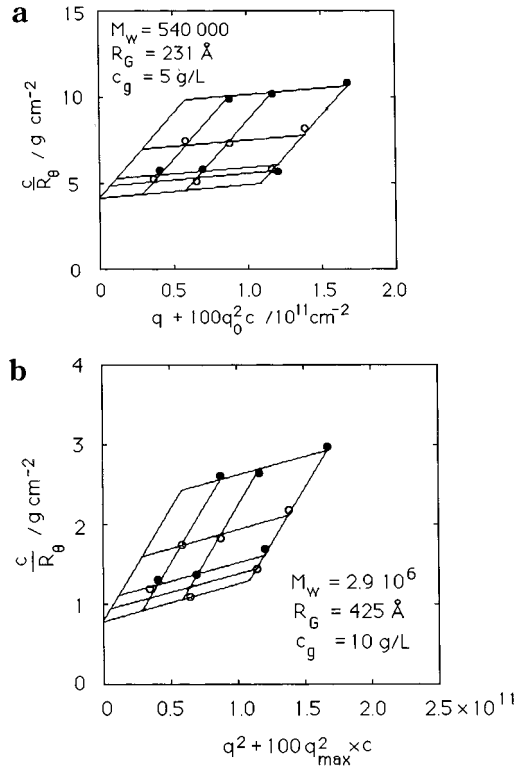

Figure 8. Zimm plots from the dynamic light scattering of dextran in agarose gels: (a) $M = 5 \times 10^5$ g mol^{-1} in a $c_g = 5$ g L^{-1} gel; (b) $M = 2 \times 10^6$ g mol^{-1} in a $c_g = 10$ g L^{-1} gel.

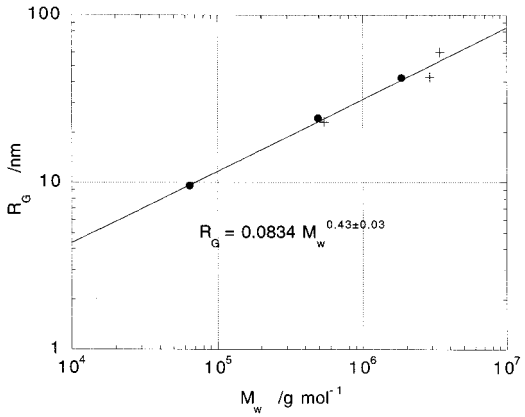

Figure 9. Plot of R_G vs M_w: filled circles, data from static light scattering (ref 10); crosses, dynamic light scattering (this work). Continuous line shown is the least-squares fit through all the data points.

for $M_w = 5 \times 10^5$ and 2×10^6 g L^{-1}, respectively. For the $M_w = 7 \times 10^4$ sample the signal-to-noise ratio was too poor to extract useful information. The resulting molecular parameters are listed in Table 1. Figure 9 shows that the values of R_G, plotted as a function of M_w, fall on a straight line that is consistent with previous static light scattering measurements on the same dextran molecules in free solution.[10]

The light scattering measurements of ref 10 for dextran in free solution give for the ratio of the radius of gyration to the hydrodynamic radius $\rho = R_G/R_H \approx 1.5$, the value expected theoretically for a linear polymer at the Θ condition. For the highest molar mass sample, however, this ratio is even smaller, a result that is probably due to the well-known phenomenon of branching in this polymer.[18] For the present measurements of dextran in agarose gels, the dynamic scattering results for the high molar mass sample M_w depend somewhat on the agarose concentration; bearing in mind that these results form a master curve in Figure 9, however, these differences are probably real and may reflect fractionation of the dextran with increasing gel concentration, i.e., larger masses are immobilized as the pore size decreases. For the gel at $c_g = 10$ g L^{-1}, the apparent ratio ρ for the dextran in this sample turns out to be smaller than that of an impenetrable uniform sphere ($\rho_{sphere} = (3/5)^{1/2}$). Such an apparently unphysical result can be explained by entanglements acting between dextran molecules and the matrix: as the radius of gyration becomes comparable with the pore size of the matrix, entanglements hinder the motion of the dextran and the apparent value of R_H becomes anomalously high. This conclusion is also in agreement with the anomalous variation of D_zR_θ mentioned above.

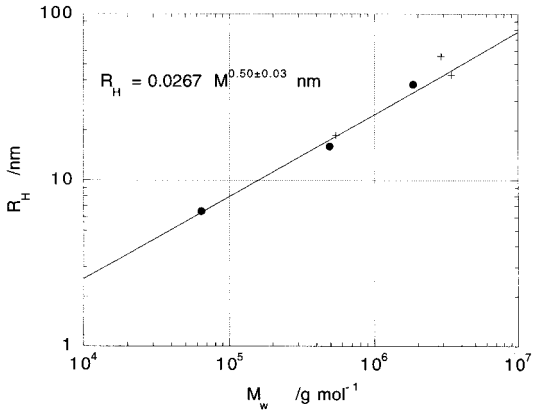

Figure 10. Plot of the hydrodynamic radius R_H vs M_w: filled circles, data from ref 10; crosses, this work. Continuous line shown is the least-squares fit through all the data points except that from the 10 g L^{-1} gel (topmost point in the graph), owing to possible entanglement effects.

The power law exponent appearing in Figure 9, $\nu = 0.43 \pm 0.03$, is significantly lower than that expected for a linear polymer in a good solvent ($\nu = 0.588$) or even that for a Θ solvent ($\nu = 0.5$). From Table 1, however, it can be seen that the second virial coefficient A_2 is small but positive. Water is therefore a good solvent, a result that is in agreement with the positive slope of $D_z(c)$ visible in Figure 5, but inconsistent with the Θ-like (or poor solvent-like) values of ρ. These results can be understood if it is assumed that the dextran samples exhibit a partially branched character.

Finally, in Figure 10 the molar mass dependence of R_H is plotted together with the results of ref 10. The least-squares fit shown excludes the datum point from the $c_g = 10$ g L^{-1} sample since it is perturbed by the effect of entanglement. Acceptable agreement is found with a power law fit of exponent $\nu_{dyn} = 0.50 \pm 0.03$. In contrast to linear polymers,[19] this value exceeds that of the static exponent ν, but it is still much lower than that for linear polymers in a good solvent. From Figures 9 and 10 it follows that the ratio ρ is a decreasing function of molar mass. We therefore conclude, once again, that the dextran molecules have a branched structure.

It is remarkable that the above measurements show no evidence for shrinkage of the dextran molecules inside the network as a result of the reduction in configuration space, as expected theoretically[20] and observed experimentally in other systems:[21,22] indeed, the values of R_G of the dextran inside the gel lie on the same master curve as for the free solution. Our interpretation of this result is that, during the formation of the agarose gels, competition between the agarose and dextran molecules ensures that the available space is sufficient for their effective radius not to be significantly diminished. This situation is the opposite of that prevailing in the previous experiments, where the configuration of the networks was established prior to the introduction of the guest polymer.[21,22]

Conclusions

The dynamic light scattering observations described here show that it is possible to measure the properties of large molecules moving inside a rigid matrix that scatters light much more strongly than the molecules themselves. In particular, measurements can be made not only of the hydrodynamic radius but also of the molar mass and radius of gyration of the dissolved molecules.

The present observations confirm our previous finding that the reduction of the translational diffusion coefficient is caused by a reduction of the osmotic pressure of the dextran inside the restricted geometry of the agarose matrix. For the higher molar masses investigated here, however, an additional slowing effect is observed, which is attributed to entanglements between the dextran and the agarose network. It is also concluded that the dextran displays a branched structure.

Acknowledgment. Carmen Kloster thanks the CAPES Foundation of the Ministry of Education of Brazil for financial support. Financial support from Fapergs and CNPq is also acknowledged. We are grateful to R. Armisen of Hispanagar, Spain, for supplying the agarose and to Redouane Borsali and to Anne-Marie Hecht for enlightening discussions. This work was performed as part of a sandwich thesis under an agreement between the University Joseph Fourier of Grenoble, France, and the Universidade Federal do Rio Grande do Sul, Porto Alegre, Brazil.

References and Notes

(1) Langevin, D.; Rondelez, F. *Polymer* **1978**, *19*, 875.
(2) Allain, C.; Drifford, M.; Gauthier-Manuel, B. *Polymer* **1986**, *27*, 177.
(3) Nishio, I.; Reina, J. C.; Bansil, R. *Phys. Rev. Lett.* **1987**, *59*, 684.
(4) Pu, Z.; Brown, W. *Macromolecules* **1989**, *22*, 890.
(5) Won, J.; Onyenemezu, C.; Miller, W. G.; Lodge, T. P. *Macromolecules* **1994**, *27*, 7389.
(6) Kuo, C.-S.; Bansil, R.; Koňák, C. *Macromolecules* **1995**, *28*, 768.
(7) Ye, X.; Tong, P.; Fetters, L. J. *Macromolecules* **1998**, 31, 5785.
(8) Shibayama, M.; Isaka, Y.; Shiwa, Y. *Macromolecules* **1999**, *32*, 7086.
(9) Kloster, C.; Bica, C.; Lartigue, C.; Rochas, C.; Samios, D.; Geissler, E. *Macromolecules* **1998**, *31*, 7712.
(10) Roger, P. Thesis, University of Nantes, France, 1993.
(11) Berne, B. J.; Pecora, R. *Dynamic Light Scattering;* Wiley: New York, 1976.
(12) Sellen, D. B. *J. Polym. Sci., Part B: Polym. Phys.* **1987**, *25*, 699.
(13) Joosten, J. G. H.; McCarthy, J. L.; Pusey, P. *Macromolecules* **1991**, *24*, 6691.
(14) Landau, L. D.; Lifschitz, E. M. *Fluid Mechanics*; Pergamon: Oxford, 1959.
(15) de Gennes, P. G. *Scaling Concepts in Polymer Physics*; Cornell University Press: Ithaca, NY, 1979.
(16) Righetti, P. G.; Brost, B. C. W.; Snyder, R. S. *J. Biochem. Biophys. Methods* **1981**, *4*, 347.
(17) Rochas, C.; Hecht, A. M.; Geissler, E. *Macromol. Symp.* **1999**, *138*, 157.
(18) Kuge, T.; Kobayashi, K.; Kitamura, S.; Tanahashi, H. *Carbohydr. Res.* **1987**, *160*, 205.
(19) Adam, M.; Delsanti, M. *Macromolecules* **1977**, *10*, 1229.
(20) Baumgärtner, A.; Muthukumar, M. *J. Chem. Phys.* **1987**, *87*, 3082.
(21) Horkay, F.; Stanley, H. B.; Geissler, E.; King, S. M. *Macromolecules* **1995**, *28*, 678.
(22) Briber, R. M.; Liu, X.; Bauer, B. J. *Science* **1995**, *268*, 395.

MA992005Q